



Universiteit
Leiden
The Netherlands

Local effects of immunosuppressants in the skin and impact on UV carcinogenesis

Voskamp, P.

Citation

Voskamp, P. (2012, May 9). *Local effects of immunosuppressants in the skin and impact on UV carcinogenesis*. Retrieved from <https://hdl.handle.net/1887/18930>

Version: Corrected Publisher's Version

License: [Licence agreement concerning inclusion of doctoral thesis in the Institutional Repository of the University of Leiden](#)

Downloaded from: <https://hdl.handle.net/1887/18930>

Note: To cite this publication please use the final published version (if applicable).

Cover Page



Universiteit Leiden



The handle <http://hdl.handle.net/1887/18930> holds various files of this Leiden University dissertation.

Author: Voskamp, Pieter

Title: Local effects of immunosuppressants in the skin and impact on UV carcinogenesis

Date: 2012-05-09

Chapter 2

Early and late effects of the immunosuppressants rapamycin and mycophenolate mofetil on UV carcinogenesis

De Gruijl FR, Koehl GE, Voskamp P, Strik A, Rebel HG, Gaumann A, De Fijter JW, Tensen CP, Bouwes Bavinck JN, Geissler EK

Int J Cancer. 2010 Aug 15;127(4):796-804.

Abstract

Increased skin cancer risk in organ transplant recipients has been experimentally emulated with enhanced UV carcinogenesis from administering conventional immunosuppressants. However, a newer generation immunosuppressive drugs, rapamycin (Rapa) and mycophenolate mofetil (MMF), have been shown to impair angiogenesis and outgrowth of tumor implants. To ascertain the overall effect on UV carcinogenesis, Rapa and MMF were admixed into the food-pellets of hairless SKH1 mice receiving daily sub-sunburn UV dosages. With immunosuppressive blood levels neither of the drugs affected onset of tumors (<2mm), but in contrast to MMF, Rapa significantly increased latency of large tumors (≥ 4 mm, medians of 190 vs 125 days) and reduced their multiplicity (1.6 vs 4.5 tumors per mouse at 200 days). Interestingly, tumors (>2mm) from the Rapa-fed group showed a reduction in UV-signature *p53* mutations (39% vs 90%) in favor of mutations from putative base oxidation. This shift in mutation spectrum was not essentially linked to the reduction in large tumors as it was absent in large tumors similarly reduced in number when feeding Rapa in combination with MMF, possibly owing to an antioxidant effect of MMF. Significantly fewer tumor cells were Vegf-positive in the Rapa-fed groups, but a correspondingly reduced expression of Hif-1 α target genes (*Vegf*, *Ldha*, *Glut1*, *Pdk1*) that would indicate altered glucose metabolism with increased oxidative stress was not found. Remarkably, we observed no effect of the immunosuppressants on UV-induced tumor onset, and with impaired tumor outgrowth Rapa could, therefore, strongly reduce skin carcinoma morbidity and mortality in organ transplant recipients.

Introduction

One of the most remarkable feats of modern Western medicine in the last century has undoubtedly been organ transplantation. However, as the initially leading mortality from immunologic and non-immunologic graft failure diminished and life expectancy of organ transplant recipients increased, other complications have risen. A major complication, which worsens as the graft survival is extended, is posttransplant malignancy, among which skin carcinomas are most prominent^{1,2}. The carcinomas tend to be more aggressive in organ transplant recipients, causing substantial mortality³, and the abundance of precursor lesions (actinic keratoses) can have serious blemishing effects.

Skin carcinomas among white Caucasians are clearly related to solar UV exposure⁴, and so are the skin carcinomas in organ transplant recipients^{2,5}, as reflected by predominant occurrence in sun-exposed skin. A striking observation is that the ratio of squamous cell carcinoma (SCC) over basal cell carcinoma (BCC) in the general population ranges around 1:3, whereas the ratio is reversed in organ transplant recipients. In the Netherlands it was estimated that about 40% of the renal transplant recipients will have contracted at least one skin carcinoma by 20 years after transplantation⁶; in Australia this percentage is already exceeded after 9 years⁷.

From classic animal experiments it is known that UV-induced skin cancers are antigenic and subject to elimination by the immune system, but a sub-carcinogenic course of UV irradiations can suppress the rejection and even induce specific tolerance toward the tumor⁸. Hence, the dramatic increase of skin carcinomas in immune suppressed allograft recipients was immediately attributed to the lack of adequate cellular immunity directed against the skin carcinomas. Experiments by Australian groups^{9,10} confirmed that the immunosuppressants azathioprine and cyclosporine sped up UV carcinogenesis in a hairless mouse model. However, Kelly et al. also showed that these classical immunosuppressants adversely affected repair of UV-induced DNA damage in skin cells¹¹. Moreover, this group recognized that azathioprine led to photosensitization of the DNA to long wavelength UV-A radiation, thus increasing the DNA damage caused by (solar) UV exposure¹². This photosensitization has been confirmed and studied in greater detail more recently¹³. Besides lowering DNA repair, cyclosporine was found to impair apoptotic responses to UV irradiation in BALB/c mice¹⁴, and these disruptive effects from calcineurin inhibitors, like cyclosporine, were confirmed in human keratinocytes¹⁵. Aside from immunosuppression *per se*, these drug-specific adverse effects from classical immunosuppressants on skin cells are bound to increase the skin carcinoma risk related to (solar) UV exposure.

A new generation of immunosuppressants may not have these drawbacks. In contrast to the traditional immunosuppressants, mycophenolate mofetil (MMF) and rapamycin (Rapa) impair the outgrowth of tumor inoculations¹⁶⁻¹⁹. Although MMF (or rather its metabolite mycophenolic acid), like azathioprine, interferes with purine synthesis, MMF does not give rise to incorporation of (6-thio-guanine) pseudo-bases that photosensitize DNA. Furthermore, Rapa operates through an entirely different mechanism, by blocking mTor (mammalian target of rapamycin) up-stream from 4Ebp1 and S6K in the Akt 'survival pathway'²⁰, thus regulating translation. The anti-angiogenic effect of Rapa is linked to both a reduction in production of Vegf-a in tumor cells and a diminished endothelial response¹⁷. Transcription of Vegf-a can be driven by Hif-1 α which in turn is under translational control of mTor²¹⁻²⁴. Furthermore, Rapa reportedly causes apoptosis in p53-null cells²⁵ and impairs tumor outgrowth in p53-null mice²⁶. As skin carcinomas raised by chronic UV exposure show an abundance of p53 mutations²⁷ one might expect a Rapa-driven selective apoptotic response in these p53-mutant cells, which could lower the initiation rate of UV-induced skin carcinomas.

Considering these important differences between classical and novel immunosuppressants, a systematic approach to assess the skin carcinoma risk in appropriate models appears to be urgently needed. Here, we pose the question of how MMF and Rapa would affect the overall process of UV carcinogenesis. Both MMF and Rapa are expected to impair the outgrowth of UV-induced primary skin tumors, but Rapa may also lower the rate of initiation of these tumors. A net beneficial effect would distinguish these novel suppressants from azathioprine and cyclosporine, which have been shown to enhance UV carcinogenesis in experiments with immunocompetent hairless mice¹⁰. Using the same hairless mouse model, we assessed the effect of Rapa and MMF treatment on UV carcinogenesis.

Materials and Methods

The mice

SKH-1 hairless mice (Charles River, Maastricht, The Netherlands) entered the experiment at 8 weeks of age; both male and female mice were used. The animal room was illuminated with yellow fluorescent tubes (Philips TL40W/16, Eindhoven, The Netherlands) that did not emit any measurable UV radiation. The animals were housed individually in Macrolon type 1 cages (Techniplast, Bugguggiate, Italy) under a 12 h light-12 h dark cycle at 23°C, 60% humidity. Standard chow was supplied in ample amounts (55-60 g/mouse/week), and drinking water was available *ad libitum*. Cage enrichment was absent to prevent shielding

of the animals from UV exposure. All experiments were performed in accordance with legislation and approval of the medical center's ethics committee.

Groups on diets with admixtures of Rapa and MMF

To avoid repeated i.p. injections of the immunosuppressants, exploratory experiments with admixtures of the drugs to standard mouse chow were performed²⁶. For the present experiment *ssniff GmbH* (Soest, Germany) supplied the food with Rapa at 20 mg/kg and MMF at 660 mg/kg. Four diet groups were formed: Rapa (n=10), MMF (n=10), Rapa and MMF (n=12) and a control group (n=10) fed the standard chow without admixtures. No apparent differences in food intake were observed between the four groups. With roughly 50 g/wk of food intake by a 30 g mouse, we estimated a weekly intake of Rapa at about 30 mg/kg and MMF at about 1 g/kg. All diets stocks were refrigerated to inhibit degradation.

UV irradiation

The four groups were started on their respective diets 1 week before subjecting them to a regimen of daily UV exposure. TL-12/40W tubes (Philips, Eindhoven, The Netherlands; 54% output in UVB – 280 to 315 nm – and 46% output in UVA – 315 to 400 nm) were used for daily UV exposure. The lamps were mounted over the cages with grid covers to allow undisturbed exposure of the mice. The lamps were automatically switched on daily from 12.30 to 12.50 h. The threshold dose for a sunburn reaction (minimal edemal dose, MED) in the hairless SKH-1 mouse was $\sim 500 \text{ J/m}^2$ UV under these lamps. The lamps were dimmed both electronically and by insertion of perforated metal sheets to expose the mice daily to 250 J/m^2 of UV radiation (0.5 MED).

Tumor assessment

The mice were inspected weekly for tumors which were registered for each mouse individually on maps (thus recording location, size, form and coloration/vascularisation). First smallest perceptible (<1 mm in diameter) lesion had to be observed at least in two successive checkups to be confirmed and counted. Upon removal of animals from the experiment, tumors were isolated from animals of each group for further analysis as described below.

Histology and Immunohistochemistry

All stainings were performed on formalin-fixed and paraffin-embedded sections (5 μm) of skin containing tumors. Hematoxylin and eosin (H&E) staining was performed for tumor staging. The following antibodies were used for immunohistochemistry: rat anti-mouse Vegf-a antibody (RELIATech, Braunschweig, Germany), rabbit anti-Hif-1 α (Novus, Littleton/CO,

USA), rabbit anti-phospho-4Ebp1 (Thr 37/46, 236B4; Cell Signaling, Danvers/MA, USA), rabbit anti-phospho-S6 ribosomal protein (Ser235/236, 91B2; Cell Signaling, Danvers/MA, USA), rat anti-mouse CD34 (clone MEC 14.7; Acris Antibodies, Herford, Germany), using standard protocols and detection by diaminobenzidine. Staging and (immune-)histological evaluation of tumors from each group were performed by a blinded pathologist (Dr. A. Gaumann, University of Regensburg) who is experienced in mouse and human pathology, including diagnosis of actinic keratoses as proper precursors of squamous cell carcinomas²⁸.

RNA and cDNA preparation

Excised samples of tumors, non-tumor dorsal skin, and ventral skin were treated with RNAlater-ICE (Ambion), snap-frozen in liquid nitrogen and stored in a freezer at -80°C. A biopsy of maximally 8 mm³ in volume was taken from every tumor by manual excision under a stereomicroscope. The biopsies were homogenized using a rotor stator homogenizer (Ultra-Turrax T8, IKA, Staufen, Germany), followed by RNA extraction with RNeasy mini kit (Qiagen, Valencia, Ca, USA). 0.5µg of total RNA was reverse-transcribed using the iScript cDNA Synthesis kit (Bio-Rad).

Mutational analysis

Tumor cDNA was used to amplify the entire coding sequences of the p53 transcript by RT-PCR in two overlapping fragments (1st amplicon with primers CCTGGCTAAAGTCTGTAGC forward and GCCTGTCTTCCAGATACTCG reverse, and 2nd amplicon with CCTGTTCATCTTTGTCCCTTC forward and GCAGAGACCTGACAACCTATC reverse). RT-PCR was performed with iQ SYBR Green SuperMix (Bio-Rad, Hercules, Ca, USA) on an iQ5 thermocycler (Bio-Rad). The reaction mixture was heated to 95°C for 3 min and amplification was carried out for 40 cycles of 95°C for 30 sec, 60°C for 30 sec and 72°C for 1 min. The RT-PCR products were completely sequenced in both directions. Cycle-sequencing was performed using ABI PRISM Big Dye Terminators v 3.1 Cycle Sequencing Kit (Applied Biosystems, Foster city, Ca, USA) and sequencing products were run on an ABI PRISM 3730 Analyzer (Applied Biosystems). Mutation Surveyor (SoftGenetics LLC) software was used for analysis of the sequencing files.

Real-time quantitative RT-PCR analysis

Tumors, as well as dorsal and ventral skin were analyzed for *Ldha*, *Pdk1*, *Glut1*, *Vegf-a* by real-time quantitative RT-PCR²⁹ (primer pairs: TGCTCTCCAGCAAAGACTACTGT forward, GACTGTACTTGACAATGTTGGGA reverse for *Ldha*; AGGCGGCTTTGTGATTTGTATTATG forward, TGTATTGTCTGTCTCTGGTGATTTCG reverse for *Pdk1*; GGGCTGCCAGGTTCTAGTC forward,

CCTCCGAGGTCCTTCTCA reverse for *Glut1*; AAGGAGAGCAGAAGTCCCATGA forward, CACAGGACGGCTTGAAGATGT reverse for *Vegf-a*)³⁰. β -actin was used as the cellular housekeeping gene for normalization³¹. PCR reaction settings were 95 °C for 3 min, then 40 cycles at 95 °C for 15 s and 58 °C for 45 s; melting curves were also examined after each run.

Statistical tests

Kaplan Meier plots of tumor-free survival were analysed by χ^2 tests (Graphpad Prism 3.0). Differences in pair-wise comparisons of tumor yields were analysed with Mann Whitney U tests, and Univariate Analysis of Variance was used to test simultaneously for group and gender effects on tumor yields (SPSS 12.0.1). Immunohistological scores and tumor staging was analyzed by pair-wise comparisons using Mann Whitney Rank Sum tests (SigmaPlot9.0/SigmaStat3.1). Differences in p53 mutations between the diet groups were calculated by χ^2 tests. $p < 0.05$ was considered to indicate a significant difference.

Results

Response to diets

Animals in the 4 groups showed no differences in weight, and gained weight from the start of the experiment up to 16 weeks (control males from 30.0 ± 2.4 g [\pm SD] to 33.8 ± 2.9 g; females from 25.5 ± 1.6 to 27.9 ± 1.8 g). Blood levels of Rapa (33 ± 11 ng/ml, $n=6$) and MMF (mycophenolic acid at 2.9 ± 0.8 mg/l, $n=3$) were measured after 1 week on food containing the drugs, and were similar to those previously reported²⁶.

Tumors

The animals showed no signs of sunburn throughout the experiment. This regimen of daily UV exposure of hairless mice was found to induce endophytic tumors which grow out to carcinomas²⁸. Benign papillomas (exophytic – often pedunculated – cauliflower-like tumors) were a small minority (<10%). These earlier findings were confirmed by pathology on tumors from the different groups. In summary, almost all tumors larger than 4mm were (invasive) SCC, whereas a substantial proportion of smaller tumors were SCC precursors, e.g. in situ carcinomas (Figure 1). No basal cell or spindle cell carcinomas were found. Papillomas were not included in the analyses of tumor induction.

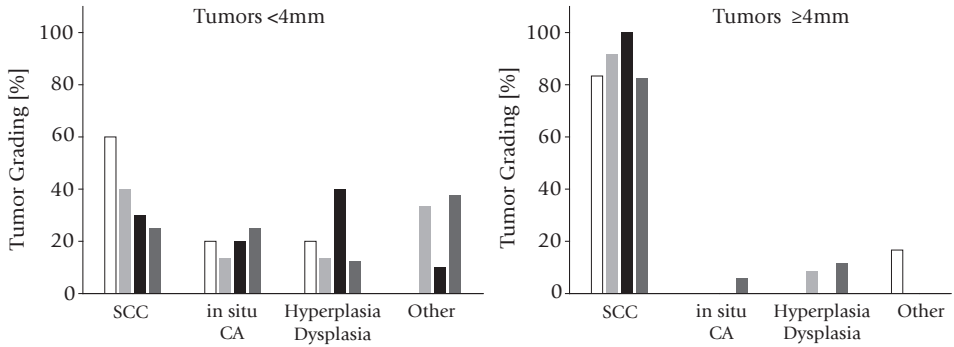


Figure 1: Histopathology of tumors smaller and larger than 4 mm in diameter; quartets of bars representing control (white bar), MMF (light gray), Rapa (black), and Rapa/MMF (dark gray) groups.

Tumor latency times

Figure 2 shows the tumor-free survival in the 4 different diet groups with tumor detection threshold set at 4 different diameters: minimal perceptible at a few tenths of a mm, 1 mm, 2mm and 4mm. No differences were evident between the four groups for tumors with diameters up to 1mm. For tumors $\geq 2\text{mm}$, the Rapa group clearly showed an increase in the time of tumor-free survival ($p=0.0025$ when compared with control). And for tumors $\geq 4\text{mm}$ the differences between the four groups are very distinct, with the control group developing the tumors most rapidly (with a median latency time, t_m , of around 125 days), followed by the MMF group ($t_m=140$ d, not significantly different from controls), the MMF/Rapa group ($t_m=170$ d, $p=0.0004$ vs controls), and, lastly, the Rapa group ($t_m=190$ d, $p=0.0021$ vs controls); i.e., the Rapa group showed a delay of about 50% when compared to the control group. No overall differences in latency times between males and females were detected ($p=0.34$).

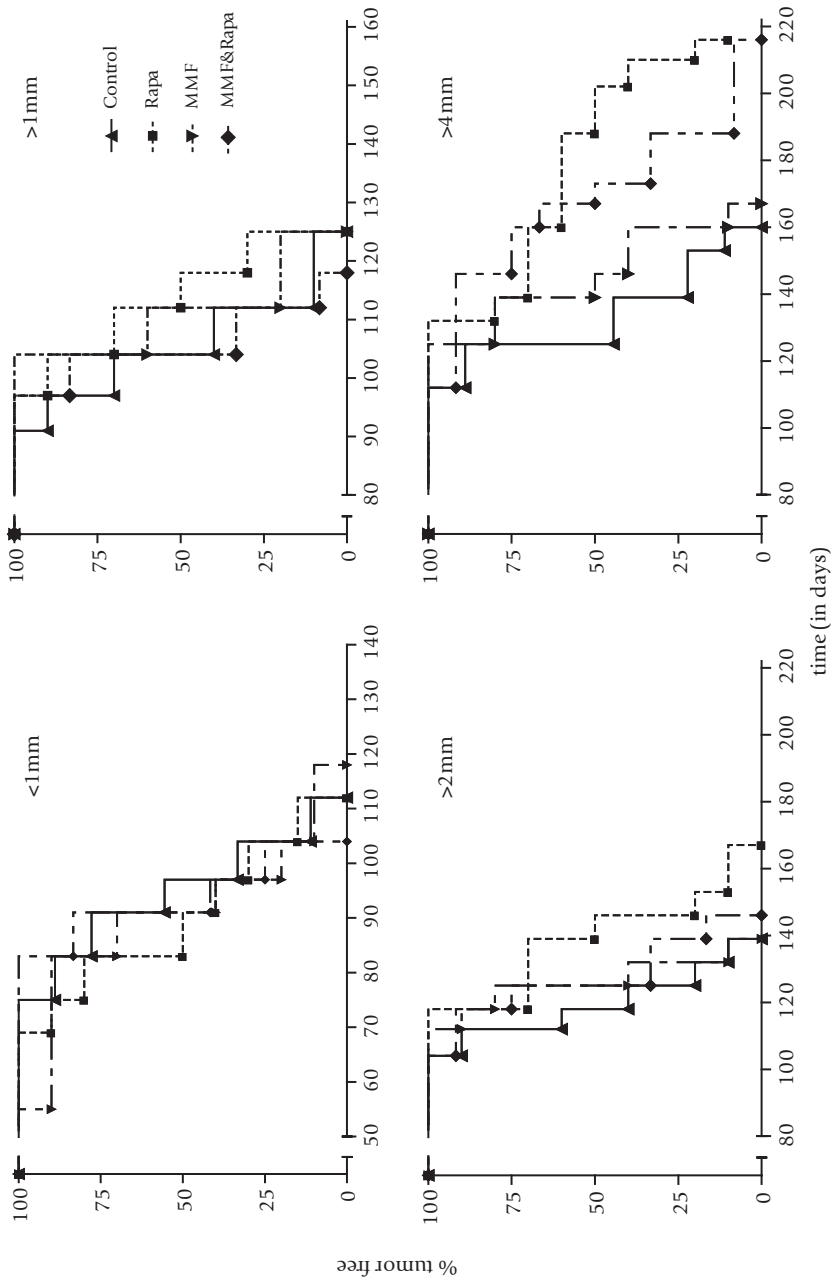


Figure 2: Kaplan Meier plots of tumor free survival in the 4 diet groups with the threshold for tumor detection set at 4 different diameters: upper left panel for minimal perceptible tumors estimated at 0.5 mm in diameter (overall no significant difference between groups), upper right panel for tumors at 1 mm (no significant difference), lower left panel for tumors at 2 mm ($p=0.0053$) and lower right panel for tumors at 4 mm in diameter ($p=0.0014$).

Tumor multiplicity

Aside from how quickly a first tumor appears, the number of tumors that an individual mouse develops is an important measure of severity. And, with small experimental groups like in the present study ($n=10-12$), counting the number of tumors increases the numerical strength of the analysis. The average number of tumors per mouse is referred to as 'tumor yield'. These yields in the 4 different diet groups are depicted in Figure 3 with the threshold for tumor detection set at 4 different diameters: either minimal perceptible at a few tenths of a mm, 1mm, 2mm or 4mm (i.e. all tumors with diameters at or over the threshold were counted).

With the tumor detection threshold set at minimal perceptible lesions no discernible differences were observed up to 130 days. For tumors ≥ 1 mm there was a significant difference at 139 days between the Rapa group and the control group (10.4 vs 19.2 tumors/mouse, $p=0.003$). For tumors ≥ 2 mm there was an even larger relative difference at that time point (1.6 vs 6.9 tumors/mouse, $p=0.002$) and at subsequent time points. The yields of the largest tumors (≥ 4 mm) showed the clearest differences. At day 202 the Rapa group had developed significantly fewer large tumors than the control group (1.6 vs 4.5 tumors/mouse, $p=0.005$), as did the Rapa/MMF combination group (1.8 vs 4.5 tumors/mouse, $p=0.007$). MMF appeared to have little effect as there was only a minor difference between the control group and the MMF group (4.5 and 3.6 tumors/mouse, respectively, n. s.), and virtually no difference between the Rapa and Rapa/MMF groups (1.6 and 1.8 tumors/mouse, n. s.). Again, no overall differences were found between males and females in tumor yields (for diameters ≥ 1 mm $p=0.35$ at day 139, and ≥ 4 mm $p=0.89$ at day 202).

Angiogenesis and Vegf-a staining

Although it has been shown that the outgrowth of implanted tumors can be hampered by an anti-angiogenic effect of Rapa or MMF^{16, 17, 26}, we could not detect any differences in the density of vessels in the tumor samples from the different groups (either by counting the number of vessels or by quantifying vessel endothelial cells stained with CD34; data not shown). Like in the tumor implants, we did, however, observe significantly less expression of Vegf-a in the tumor cells from the Rapa group (Figure 4). The tumor stroma, on the other hand, did not show any difference in Vegf-a staining (data not shown). Interestingly, at this advanced stage of tumor growth (diameters $>2-4$ mm) we could not detect any clear reduction by Rapa in the levels of activated mTor effector proteins (phospho-S6 ribosomal protein, nuclear 4Ebp1 and Hif-1 α ; data not shown) which showed substantial variation in immunohistochemical staining between the tumors.

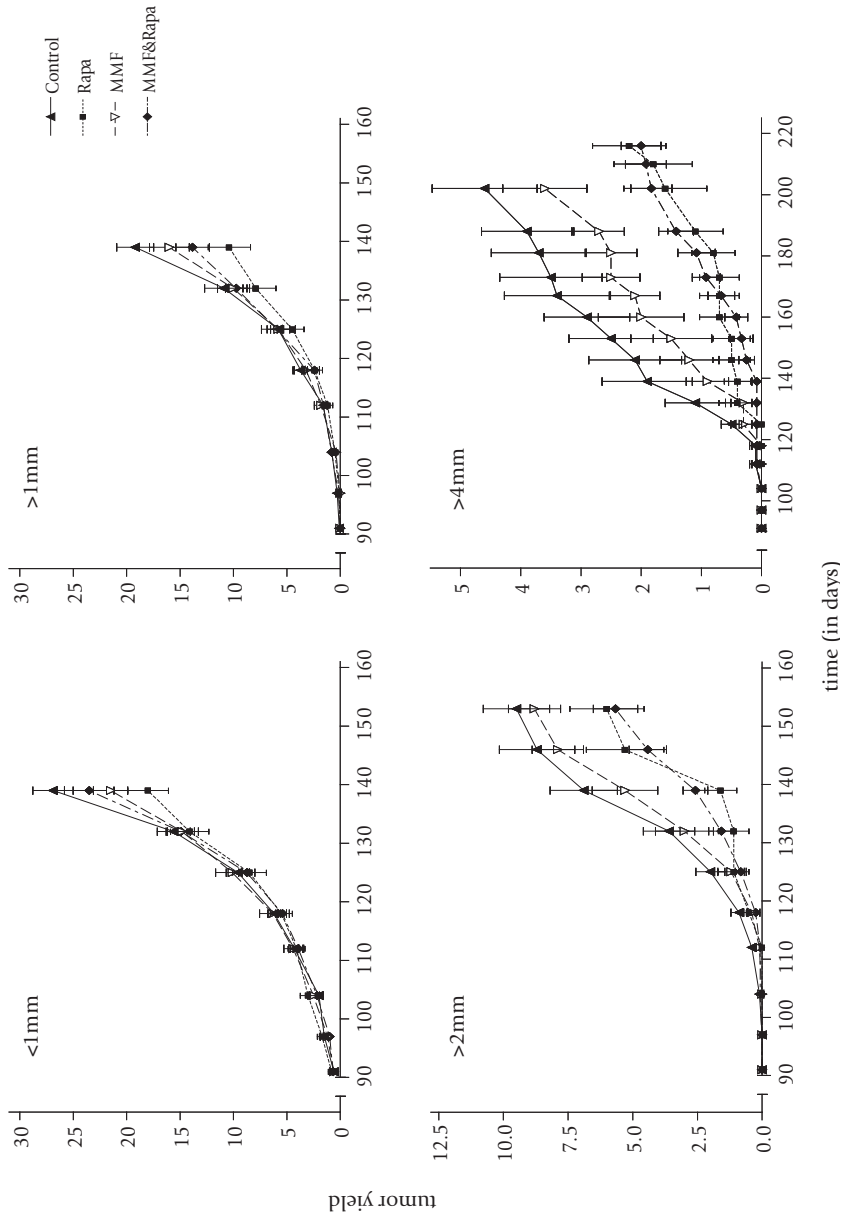


Figure 3: Plots of tumor yields in the 4 diet groups with the threshold for tumor detection set at 4 different diameters: upper left panel for minimal perceptible tumors estimated at 0.5 mm in diameter, upper right panel for tumors at 1mm, lower left panel for tumors at 2mm, and lower right panel for tumors at 4mm in diameter; whiskers depict SEM.

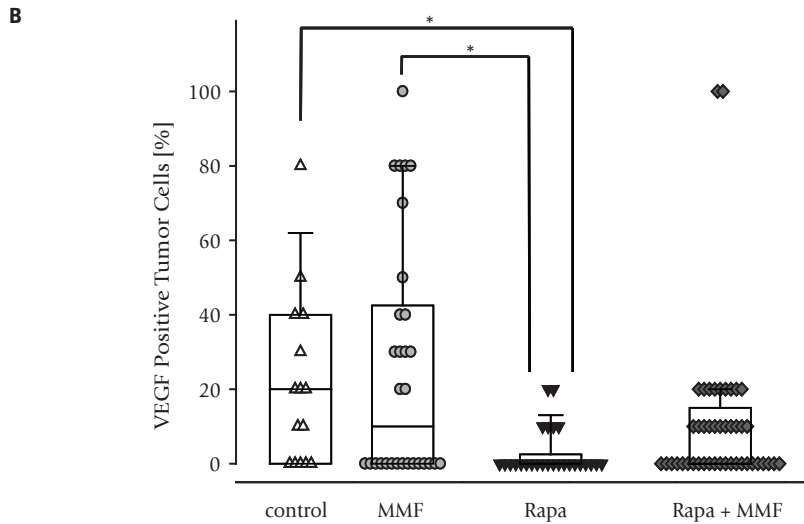
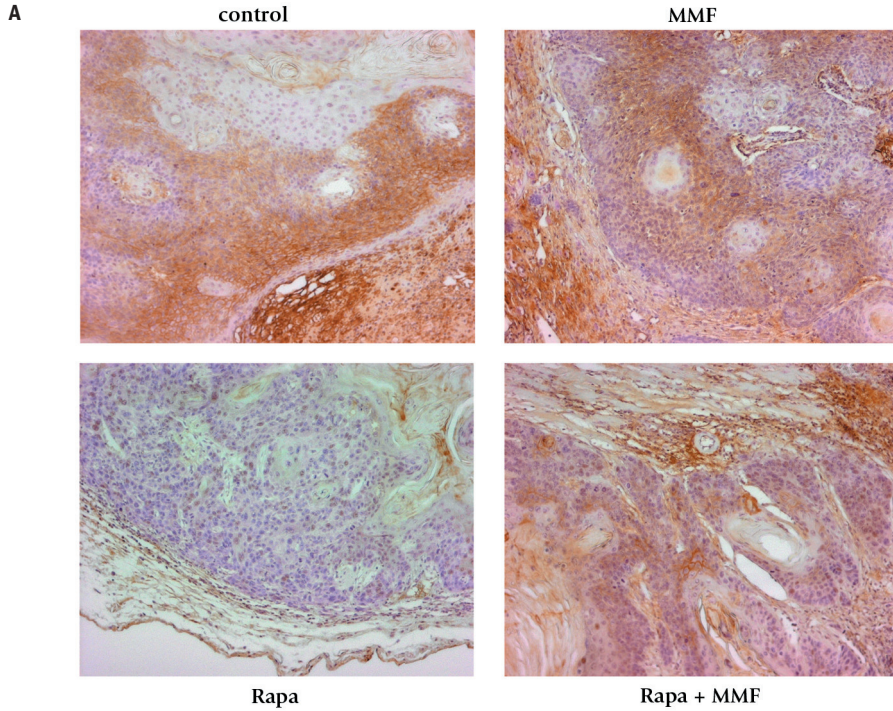


Figure 4: Vegf-a expression in tumors: (A) typical examples of tumor sections histochemically stained for Vegf-a; (B) graphical presentation of Vegf-a expression in tumors from the 4 experimental groups; * $p=0.005$ vs control.

Mutation analysis of p53 in tumors

Mutations in *p53* occur early in UV carcinogenesis and they show a UV signature, i.e., C to T transitions at dipyrimidine sites⁴. We inspected whether the immunosuppressants could have affected the *p53* mutation spectrum by metabolic effects from Rapa, or by anti-oxidant effects or effects on purine synthesis from MMF. Figure 5 gives a graphical summary of percentages of UV signature mutations in *p53* in tumors (>2mm) from the four experimental groups (table 1 gives a more detailed overview). The control group clearly showed the expected mutation pattern with predominantly UV signature mutations. The mutation spectrum from the MMF group showed no significant change. But the Rapa group showed a clear reduction in percentage of UV signature mutations (39% vs an average of 90% in the other groups, $p=0.007$ by χ^2 test). The relative increase in G>T and T>G mutations could be caused by oxidative damage³², and the T>C transitions possibly originate from thymine glycols as oxidation products³³. Interestingly, combining Rapa with MMF again produced a *p53* mutation spectrum dominated by UV signature mutations, comparable to the control group.

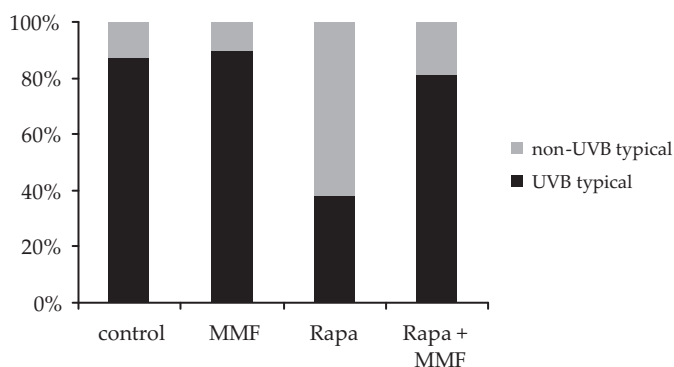


Figure 5: Graph of the percentage of UV signature mutations (C to T transition at dipyrimidine site) among the *p53* mutations in tumors from the 4 experimental groups.

The Warburg effect

A possible source of reactive oxygen could be the mitochondria by effects of Rapa on the respiration of tumor cells. Tumors have been reported to have shifted their glucose consumption from oxidative phosphorylation to aerobic glycolysis to lactate, which is dubbed the Warburg effect and can be driven by Hif-1 α ³⁴. We hypothesized that Rapa could reduce the Warburg effect by lowering the level of Hif-1 α or by interfering with Hif-1 α

activation³⁵, and thus enhance oxidative phosphorylation and the release of reactive oxygen species (ROS) from mitochondria. Therefore, we measured expression of Hif-1 α target genes³⁴: *Glut1*, *Pdk1*, *Ldha*, and *Vegf-a*, where *Glut1* is a glucose transporter, *Pdk1* blocks pyruvate's entry into the Krebs cycle, and *Ldha* catalyses the conversion of pyruvate and NADH to lactate and NAD. We found no differences between mRNA levels from these genes in tumors taken from the Rapa and control groups, as shown in Figure 6. However, we did observe interesting differences between UV-exposed skin, unexposed skin and tumors. In contrast to *Ldha* and *Vegf-a*, both *Glut1* and *Pdk1* were upregulated in UV-exposed dorsal skin when compared to unexposed ventral skin. But in the tumors *Glut1* and *Pdk1* expression was low and *Ldha* and *Vegf-a* expression was high. These data do not reflect any unison effect of Hif-1 α on the expression of these four target genes.

Table 1: Mutation analysis of p53 in tumors

Mouse #. Tumor #	Codon	Mutation	Amino acid	Not UV-typical
Control				
1.1	62	ctcCga>ctcTga	R>R/X	
1.2	82	gccCCt>gccTTt	P>P/F	
1.3	124	tCt>tTt	S>S/F	
2.1	142	tTg>tCg	L>S/L	✓
2.1	149	cctCca>cctTca	P> P/S	
3.1	149	cctCca>cctTca	P>P/S	
2.2	210	tttCgc>tttTgc	R>C	
3.2	210	tttCgc>tttTgc	R>R/C	
4.1	210	tttCgc>tttTgc	R>C	
1.2	238	tCc>tTc	S>S/F	
3.2	239	tGc>tTc	C>C/F	✓
5.1	270	gttCgt>gttTgt	R>C	
1.2	270	gttCgt>gttTgt	R>R/C	
1.3	270	gttCgt>gttTgt	R>R/C	
3.1	275	tgCct>tgCfct	P>P/S	
1.1	373	tCt>tTt	S>S/F	
Rapa				
6.1	110	ggcTtc>ggcCtc	F>L/F	✓
7.1	142	ttGtgg>ttTtgg	L>L/F	✓
8.1	210	tttCgc>tttTgc	R>C	
9.1	239	tGc>tTc	C>C/F	✓

Mouse #.	Tumor #	Codon	Mutation	Amino acid	Not UV-typical
9.1		247	cCt>cGt	P>P/R	✓
7.1		261	aacCtt>aacTtt	L>L/F	
10.1		262	cTg>cCg	L>P/L	✓
10.1		267	tTt>tCt	F>F/S	✓
7.1		270	gttCgt>gttTgt	R>R/C	
11.1		272	tgTgcc>tgGgcc	C>W/C	✓
11.1		275	cCt>cTt	P>P/L	
12.1		275	cCt>cTt	P>P/L	
10.2		intron4	AG mutant	heterozyg. del.	✓
MMF					
13.1		149	cctCca>cctTca	P>P/S	
14.1		210	tttCgc>tttTgc	R>C	
13.2		210	tttCgc>tttTgc	R>R/C	
15.1		210	tttCgc>tttTgc	R>R/C	
13.2		270	gttCgt>gttTgt	R>R/C	
13.3		270	gttCgt>gttTgt	R>R/C	
16.1		275	tgCct>tgCtct	P>S	
16.2		275	tgCct>tgCtct	P>S	
14.1		294	tgCct>tgCAct	P>T/P	✓
14.1		307	acCtgc>acTtgc	T>I/T	
MMF + Rapa					
17.1		77	accCct>accTct	P>P/S	
18.1		92	tCt>tTt	S>S/F	
19.1		95	cCt>cTt	P>P/L	
20.1		109-110	ggCTtg>ggTGtg	G>G, F>V/F	✓
18.2		149	cCa>cTa	P>P/L	
21.1		155	gtcCgc>gtcTgc	R>R/C	
19.2		175-176	caCCat>caTAat	H>H, H>N/H	✓
23.1		210	tttCgc>tttTgc	R>C	
21.1		261	aacCtt>aacTtt	L>L/F	
18.1		270	gttCgt>gttTgt	R>R/C	
22.1		270	gttCgt>gttTgt	R>R/C	
21.2		275	tgCct>tgCtct	P>P/S	
19.1		275	tgCct>tgCtct	P>P/S	
19.2			heterozyg. splicemutant	exon7-exon12	✓

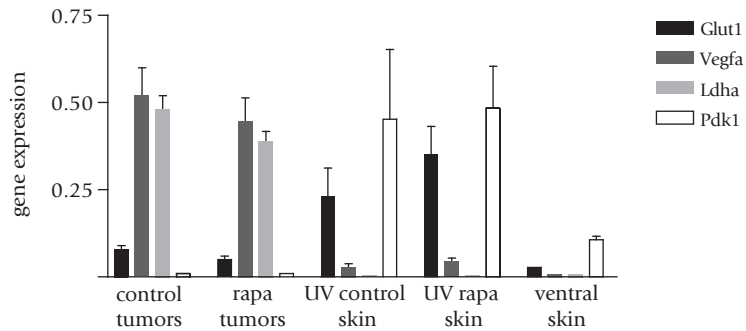


Figure 6: Expression of *Vegf-a*, *Ldha*, *Glut1* and *Pdk1* as target genes of Hif-1 α in comparison to β -*actin* in various tissue samples from Rapa-fed and control mice; error bars depict SEM (Rapa and control tumors, each n=9; UV-exposed skin from Rapa n=7 and control group n=4; unexposed control ventral skin n=3).

Discussion

In contrast to earlier findings with azathioprine and cyclosporine^{9,10}, the newer-age immunosuppressants Rapa and MMF did not enhance UV carcinogenesis. In the case of Rapa, it had the opposite effect of strongly impairing the development of large tumors (≥ 2 mm). This impairment can be attributed to the known anti-tumor, or more specifically, anti-angiogenic effects of Rapa^{16,17}. At dosages which maintained allogeneic heart grafts in mice, Rapa thus inhibited outgrowth of tumor implants whereas cyclosporine was found to enhance angiogenesis and strongly stimulate tumor outgrowth¹⁸. Rapa could even block the pro-angiogenic effect from cyclosporine. In the present study the inhibition of tumor outgrowth by Rapa appeared to be reflected in a significant reduction of Vegf-a positive tumor cells. However, the Vegf-a expression in tumor stroma did not appear to be significantly reduced, which leaves the question whether tumor cells and stroma were equally important in releasing Vegf-a into the interstitial compartment. Interestingly, we did not find any clear effect on the vasculature of tumors that grew in the Rapa-fed groups, but these tumors may be presumed to have been selected for their vascularisation and resistance to Rapa while those that lagged behind were most sensitive to the anti-angiogenic effect of Rapa. MMF was also reported to impair tumor growth and angiogenesis¹⁶, but its effect on tumor implants appeared to be highly variable, possibly owing to differences in bio-availability of its metabolite mycophenolic acid¹⁹. This may correspond to the slight – but not significant – delay in onset of tumors (≥ 2 mm) we observed in the MMF-fed animals.

Our data differ from those obtained by Duncan et al³⁶ who found that Rapa (sirolimus) increased the number of tumors by about 50% at the end of the experiment in which Rapa treatment started 10 weeks after weekly UV exposures. They reported some effects of MMF and Rapa on malignancy and average tumor size, but not any dramatic reduction in the number of large tumors, like we report here. In a subsequent study the same group did report a reduction in the number of tumors when Rapa was given after 15 weeks of UV irradiation and irradiation was discontinued³⁷; at that point the mice had already developed an average of about 5 tumors per animal. In contrast to our experiments, their experiments were not optimal to detect any effect on tumor onset. Their experimental protocols differed substantially from ours, not only in the timing UV exposures and administration of Rapa, but also in the route of applying Rapa, i.e. by i.p. injection. At effective immunosuppressive dosages (1.5 mg/kg/day), the efficacy of Rapa against tumor growth was found to be much enhanced by regular release (continuous infusion) in comparison to a massive bolus dose delivered by injection (once every 3 days)³⁸.

The concept that immunosuppressive agents should, by their very nature, enhance UV-induced skin carcinogenesis⁸⁻¹⁰ is not supported by the present experiment (nor by the aforementioned experiments in references 36 and 37). Our data show no enhancement at all from immunosuppressive dosages of MMF and Rapa, neither on early stages nor on late stages of tumor development. Early experiments did show some systemic effects on small tumors in hairless mice attributable to altered immunity: prior UV-driven induction of small tumors on a limited area of skin, speeded up later UV tumorigenesis in a distant, formerly shielded, area of skin³⁹. It should, however, be noted that the immune effects involved in UV carcinogenesis are complicated: besides a UV-induced (transient) suppression of immunisation, there is also an induction of specific tolerance toward UV-induced tumors^{8, 40-43}. UV carcinogenesis was actually delayed in CD80/CD86 double null mice lacking in tolerance induction⁴². Although immune deficient mice did develop skin tumors more rapidly upon UV exposure than their proficient counterparts, these immune deficient mice were found to develop the tumors even faster when they had been thymically-reconstituted⁴⁴. Suppression of T cell-mediated immunity can, therefore, have differential and competing effects on UV carcinogenesis, including both inhibitory and enhancing effects. Whether the lack of effect of Rapa and MMF in the present experiments on UV induction of small tumors is due to a complete lack of immunogenicity of small tumors, or whether it is due to an 'accidental' cancellation of T cell-mediated effects, remains to be determined. Although UV-induced immunosuppression has been reported to be affected by estrogen receptor

signaling⁴⁵, we have found no gender effect in our experiments, in agreement with an earlier report²⁹.

P53 mutations appear to be involved in the earlier stages of tumor development²⁷. Our suspicion that Rapa might selectively induce apoptosis in the p53-mutated cells, and thus slow down the rate at which tumors are initiated, is not supported by our data as we found no effect the onset of the smallest perceptible tumors (<1mm). To check further for local effects of the immunosuppressants on the epidermal cells that might have affected UV carcinogenesis (e.g. disturbed metabolism by Rapa) we investigated the *p53* mutation spectrum of the tumors which is normally dominated by the UV signature mutations. We found a dramatic shift in the types of mutations in tumors from the Rapa-fed group. This shift could have been due to an increase in ROS. Rapa did not cause such a shift when combined with MMF, which may be attributable to the known anti-oxidant activity of MMF.⁴⁶ We investigated the expression of target genes of Hif-1 α to ascertain whether the Warburg effect and its suppression by Rapa could be responsible for changes in oxidative stress in the tumors. Although we did not find any effect of Rapa on the expression of these four marker genes, we did find striking differences in their expression in skin depending on UV exposure and in the tumors. In UV-exposed skin, the *Pdk1* expression was increased, which implies a block of pyruvate entry into the Krebs cycle, shutting down oxidative phosphorylation and associated ROS formation in the mitochondria. Moreover, the increase in *Glut1* may be related to anti-oxidant effects by transport of vitamin C⁴⁷. We found *Ldha* to be highly expressed in the tumors which indicated that the Warburg effect was probably operative as *Ldha* catalyzes the conversion of pyruvate to lactate. Since *Pdk1* expression was low in the tumors from the control and Rapa groups, oxidative phosphorylation may also have been active in the tumors, which may thus have switched on both glucose-metabolizing pathways.

In conclusion, the present experimental data show that immunosuppressants do not necessarily enhance UV carcinogenesis, and can even lower the tumor burden. It has been already demonstrated that Rapa can impair the outgrowth of tumor implants, but our data provide evidence of the same effect on primary skin carcinomas induced by chronic UV exposure. Clinical data are beginning to emerge that also point to a lowered cancer risk when immunosuppressive medication is switched to Rapa⁴⁸⁻⁵⁰. Hence, further experimentation is urgently called for to better understand the pro- and anti-carcinogenic effects of various immunosuppressants, and eventually, to apply adequate immunosuppressive regimens while minimizing the long-term carcinogenic risk in organ transplant recipients.

Acknowledgements

We would like to thank Astrid Schwend and Cornelia Michl for technical assistance with immunohistology.

References

1. Hiesse C, Rieu P, Kriaa F, Larue JR, Goupy C, Neyrat N, Charpentier B. Malignancy after renal transplantation: analysis of incidence and risk factors in 1700 patients followed during a 25-year period. *Transplant Proc* 1997;29:831-3.
2. Fortina AB, Caforio AL, Piaserico S, Alaibac M, Tona, F, Feltrin G, Livi U, Peserico A. Skin cancer in heart transplant recipients: frequency and risk factor analysis. *J Heart Lung Transplant* 2000;19:249-5.
3. Buell JF, Hanaway MJ, Thomas M, Alloway RR, Woodle ES. Skin cancer following transplantation: the Israel Penn International Transplant Tumor Registry experience. *Transplant Proc* 2005;37:962-3.
4. De Gruijl FR. Skin cancer and solar UV radiation. *Eur J Cancer* 1999;35:2003-9.
5. Bavinck JN, De Boer A, Vermeer BJ, Hartevelt MM, van der Woude FJ, Claas FH, Wolterbeek R, Vandenbroucke JP. (1993) Sunlight, keratotic skin lesions and skin cancer in renal transplant recipients. *Br J Dermatol* 1993;129:242-9.
6. Hartevelt MM, Bavinck JN, Kootte AM, Vermeer BJ, Vandenbroucke JP. Incidence of skin cancer after renal transplantation in The Netherlands. *Transplantation* 1990;49:506-9.
7. Hardie IR, Strong RW, Hartley LC, Woodruff P, Clunie GJ. Skin cancer in Caucasian renal allograft recipients living in a subtropical climate. *Surgery* 1980;87:177-83
8. Fisher MS, Kripke ML. Systemic alteration induced in mice by ultraviolet light irradiation and its relationship to ultraviolet carcinogenesis. 1977. *Bull World Health Organ* 2002;80:908-12
9. Reeve VE, Greenoak GE, Gallagher CH, Canfield PJ, Wilkinson FJ. Effect of immunosuppressive agents and sunscreens on UV carcinogenesis in the hairless mouse. *Aust J Exp Biol Med Sci* 1985;63:655-65.
10. Kelly GE, Meikle W, Sheil AG. Effects of immunosuppressive therapy on the induction of skin tumors by ultraviolet irradiation in hairless mice. *Transplantation* 1987;44:429-34.
11. Kelly GE, Meikle W, Sheil AG. Scheduled and unscheduled DNA synthesis in epidermal cells of hairless mice treated with immunosuppressive drugs and UVB-UVA irradiation. *Br J Dermatol* 1987;117:429-40.
12. Kelly GE, Meikle WD, Moore DE. Enhancement of UV-induced skin carcinogenesis by azathioprine: role of photochemical sensitisation. *Photochem Photobiol* 1989;49:59-65.
13. O'Donovan P, Perrett CM, Zhang X, Montaner B, Xu YZ, Harwood CA, McGregor JM, Walker SL, Hanaoka F, Karran P. Azathioprine and UVA light generate mutagenic oxidative DNA damage. *Science* 2005; 309:1871-4.
14. Sugie N, Fujii N, Danno K. Cyclosporin-A suppresses p53-dependent repair DNA synthesis and apoptosis following ultraviolet-B irradiation. *Photodermatol Photoimmunol Photomed* 2002;18:163-8.
15. Yarosh DB, Pena AV, Nay SL, Canning MT, Brown DA. Calcineurin inhibitors decrease DNA repair and apoptosis in human keratinocytes following ultraviolet B irradiation. *J Invest Dermatol* 2005;125:1020-5.

16. Tressler RJ, Garvin LJ, Slate DL. Anti-tumor activity of mycophenolate mofetil against human and mouse tumors in vivo. *Int J Cancer* 1994;57:568-73.
17. Guba M, von Breitenbuch P, Steinbauer M, Koehl G, Flegel S, Hornung M, Bruns CJ, Zuelke C, Farkas S, Anthuber M, Jauch KW, Geissler EK. Rapamycin inhibits primary and metastatic tumor growth by antiangiogenesis: involvement of vascular endothelial growth factor. *Nat Med* 2002;8:128-35.
18. Koehl GE, Andrassy J, Guba M, Richter S, Kroemer A, Scherer MN, Steinbauer M, Graeb C, Schlitt HJ, Jauch KW, Geissler EK. Rapamycin protects allografts from rejection while simultaneously attacking tumors in immunosuppressed mice. *Transplantation* 2004;77:1319-26.
19. Koehl GE, Wagner F, Stoeltzing O, Lang SA, Steinbauer M, Schlitt HJ, Geissler EK. Mycophenolate mofetil inhibits tumor growth and angiogenesis in vitro but has variable antitumor effects in vivo, possibly related to bioavailability. *Transplantation* 2007;83:607-14.
20. Wan YS, Wang ZQ, Shao Y, Voorhees JJ, Fisher GJ. Ultraviolet irradiation activates PI 3-kinase/AKT survival pathway via EGF receptors in human skin in vivo. *Int J Oncol* 2001;18:461-6.
21. Lang SA, Gaumann A, Koehl GE, Seidel U, Bataille F, Klein D, Ellis LM, Bolder U, Hofstaedter F, Schlitt HJ, Geissler EK, Stoeltzing O. Mammalian target of rapamycin is activated in human gastric cancer and serves as a target for therapy in an experimental model. *Int J Cancer* 2007;120:1803-10.
22. Bernardi R, Guernah I, Jin D, Grisendi S, Alimonti A, Teruya-Feldstein J, Cordon-Cardo C, Simon MC, Rafii S, Pandolfi PP. PML inhibits HIF-1alpha translation and neoangiogenesis through repression of mTOR. *Nature* 2006;442:779-85.
23. Amornphimoltham P, Patel V, Leelahavanichkul K, Abraham RT, Gutkind JS. A retroinhibition approach reveals a tumor cell-autonomous response to rapamycin in head and neck cancer. *Cancer Res* 2008;68:1144-53.
24. Knaup KX, Jozefowski K, Schmidt R, Bernhardt WM, Weidemann A, Juergensen JS, Warnecke C, Eckardt KU, Wiesener MS. Mutual regulation of hypoxia-inducible factor and mammalian target of rapamycin as a function of oxygen availability. *Mol Cancer Res* 2009;7:88-98.
25. Huang S, Liu LN, Hosoi H, Dilling MB, Shikata T, Houghton PJ. p53/p21(CIP1) cooperate in enforcing rapamycin-induced G(1) arrest and determine the cellular response to rapamycin. *Cancer Res* 2001;61:3373-81.
26. Koehl GE, Gaumann A, Zuelke C, Hoehn A, Hofstaedter F, Schlitt HJ, Geissler EK. Development of de novo cancer in p53 knock-out mice is dependent on the type of long-term immunosuppression used. *Transplantation* 2006;82:741-8.
27. Rebel H, Kram N, Westerman A, Banus S, van Kranen HJ, de Gruijl FR. Relationship between UV-induced mutant p53 patches and skin tumours, analysed by mutation spectra and by induction kinetics in various DNA-repair-deficient mice. *Carcinogenesis* 2005;26:2123-30.
28. De Gruijl FR, van der Meer JB, van der Leun JC. Dose-time dependency of tumor formation by chronic UV exposure. *Photochem Photobiol* 1983;37:53-62.
29. El Filali M, Homminga I, Maat W, van der Velden PA, Jager MJ. Triamcinolone acetonide and anecortave acetate do not stimulate uveal melanoma cell growth. *Mol Vis* 2008;14:1752-9.

30. Huang Y, Hickey RP, Yeh JL, Liu D, Dadak A, Young LH, Johnson RS, Giordano FJ. Cardiac myocyte-specific HIF-1alpha deletion alters vascularization, energy availability, calcium flux, and contractility in the normoxic heart. *FASEB J* 2004;18:1138-40.
31. Gilsbach R, Kouta M, Bonisch H, Bruss M. Comparison of in vitro and in vivo reference genes for internal standardization of real-time PCR data. *Biotechniques* 2006;40:173-7.
32. De Gruijl FR, van Kranen HJ, Mullenders LH. UV-induced DNA damage, repair, mutations and oncogenic pathways in skin cancer. *J Photochem Photobiol B* 2001;63:19-27.
33. Basu AK, Loechler EL, Leadon SA, Essigmann JM. Genetic effects of thymine glycol: site-specific mutagenesis and molecular modeling studies. *Proc Natl Acad Sci U S A* 1989;86:7677-81.
34. Denko NC. Hypoxia, HIF1 and glucose metabolism in the solid tumour. *Nat Rev Cancer* 2008;8:705-13.
35. Land SC, Tee AR. Hypoxia-inducible factor 1alpha is regulated by mammalian target of Rapamycin (mTOR) via an mTOR signalling motif. *J Biol Chem* 2007;282:20534-43.
36. Duncan FJ, Wulff BC, Tober KL, Ferketich AK, Martin J, Thomas-Ahner JM, Allen SD, Kusewitt DE, Oberyshyn TM, Vanbuskirk AM. Clinically relevant immunosuppressants influence UVB-induced tumor size through effects on inflammation and angiogenesis. *Am J Transplant* 2007;7:2693-703.
37. Wulff BC, Kusewitt DE, VanBuskirk AM, Thomas-Ahner JM, Duncan FJ, Oberyshyn TM. Sirolimus reduces the incidence and progression of UVB-induced skin cancer in SKH mice even with co-administration of cyclosporine A. *J Invest Dermatol* 2008;128:2467-2473.
38. Guba M, Koehl GE, Nepl E, Doenecke A, Steinbauer M, Schlitt HJ, Jauch KW, Geissler EK. Dosing of rapamycin is critical to achieve an optimal antiangiogenic effect against cancer. *Transpl Int* 2005;18:89-94.
39. De Gruijl FR, van der Leun JC. Follow up on systemic influence of partial pre-irradiation on UV-tumorigenesis. *Photochem Photobiol* 1983;38:381-3.
40. Kripke ML, Fisher MS. Immunologic parameters of ultraviolet carcinogenesis. *J Natl Cancer Inst* 1976;57:211-5.
41. Spellman CW, Daynes RA. Modification of immunological potential by ultraviolet radiation. II. Generation of suppressor cells in short-term UV-irradiated mice. *Transplantation* 1977;24:120-6.
42. Loser K, Scherer A, Krummen MB, Varga G, Higuchi T, Schwarz T, Sharpe AH, Grabbe S, Bluestone JA, Beissert S. An important role of CD80/CD86-CTLA-4 signaling during photocarcinogenesis in mice. *J Immunol* 2005;174:5298-305.
43. Moodycliffe AM, Nghiem D, Clydesdale G, Ullrich SE. Immune suppression and skin cancer development: regulation by NKT cells. *Nat Immunol* 2000;1:521-5.
44. Norbury KC, Kripke ML. Ultraviolet carcinogenesis in T-cell-depleted mice. *J Natl Cancer Inst* 1978;61:917-21.
45. Widyarini, S., Domanski, D., Painter, N. and Reeve, V.E. Estrogen receptor signaling protects against immune suppression by UV radiation exposure. *Proc Natl Acad Sci U S A* 2006;103:12837-42.

46. Krotz F, Keller M, Derflinger S, Schmid H, Gloe T, Bassermann F, Duyster J, Cohen CD, Schuhmann C, Klaus V, Pohl U, Stempfle H, Sohn H. Mycophenolate Acid Inhibits Endothelial NAD(P)H Oxidase Activity and Superoxide Formation by a Rac1-Dependent Mechanism. *Hypertension* 2007;49:201-8.
47. Sagun KC, Carcamo JM, Golde DW. Vitamin C enters mitochondria via facilitative glucose transporter 1 (Glut1) and confers mitochondrial protection against oxidative injury. *FASEB J* 2005;19:1657-67.
48. Stallone, G., Schena, A., Infante, B., Di Paolo, S., Loverre, A., Maggio, G., Ranieri, E., Gesualdo, L., Schena, F.P. and Grandaliano, G. Sirolimus for Kaposi 's sarcoma in renal0transplant patients. *N Engl J Med* 2005;352:1317-23.
49. Campistol JM, Eris J, Oberbauer R, Friend P, Hutchison B, Morales JM, Claesson K, Stallone G, Russ G, Rostaing L, Kreis H, Burke JT, Brault Y, Scarola JA, Neylan JF. Sirolimus therapy after early cyclosporine withdrawal reduces the risk for cancer in adult renal transplantation. *J Am Soc Nephrol* 2006;17:581-9.
50. Campistol JM. Minimizing the risk of posttransplant malignancy. *Transplantation* 2009;87(8 Suppl):S19-22.

